

# Investigation of Characteristics of Separation Zones in T-Junctions

BAHAREH PIRZADEH\*, HAMID SHAMLOO\*\*

Civil Engineering Department  
K.N Toosi University of Technology  
No.1346 Valiasr Street, Tehran  
IRAN

**Abstract:** This paper provides detail application of FLUENT-2D software in simulation of lateral intake flows. Numerical simulations undertaken in present two dimensional work use *RSM* turbulent model. Results for dimensions of separation zone were compared with Kasthuri and Pundarikanthan (1987) that a good agreement is found between them.

**Key-Words:** Open channel, Lateral Intake, Turbulence, Separation zone, Numerical modeling, Fluent

## 1 Introduction

In hydraulic and environmental engineering, one commonly comes across branching channel flows. Some of the distinctive characteristics of a dividing flow in an open channel are illustrated in Fig.1. A zone of separation near the entrance of the branch channel, a contracted flow region in the branch channel, and a stagnation point near the downstream corner of the junction can be observed. In the region downstream of the junction, along the continuous far wall, separation due to flow expansion may occur. (Ramamurthy et al. 2007)

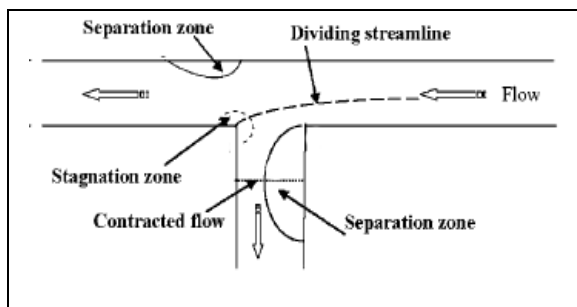


Fig.1. Flow characteristics of a dividing flow in open channels

So, flows through lateral intakes adjoining rivers and canals are turbulent. The transverse pressure gradients in the vicinity of the intake induce region of mean-velocity gradients, depth-varying surface of flow division and separation, vortices, and zone of flow reversal.

A great number of experimental and analytical studies dealt with dividing flows. Taylor (1944) conducted the first detailed experimental study in an open channel and proposed a graphical solution, which included a trial-and-error procedure. Grace and Priest (1958) presented experimental results for the division of flow at different width ratios of the branch channel orientation to the main channel. They also classified the division of flow into two regimes, with and without the appearance of local standing waves near the branch. The regime without waves corresponded to the case where the Froude numbers were relatively small, and the regime with the waves corresponded to the free over-fall conditions at sections downstream of the junction. Without the appearance of standing waves, the downstream-to-upstream depth ratio and the branch-to-downstream depth ratio are nearly equal to unity and the ratios mildly decrease while the branch-to-main channel upstream discharge ratio increases. Law and Reynolds (1966) investigated the problem of dividing flows using analytical and experimental methods. They concluded that for a dividing flow at low Froude numbers in a right-angled dividing flow, the momentum and energy principles can both be applied to describe the flow in the main channel extension.

Existing results (Krishnappa and Seetharamiah 1963; Law 1965; Sridharan 1966; Ramamurthy and Satish 1988) indicate that the flow condition at the entrance to the branch is generally unsubmerged when the Froude number  $F_r$  in the branch is greater

than a threshold value (0.3 or 0.35). This feature becomes important in correlating discharge distribution with the other flow parameters. When the flow at the section of maximum contraction is un-submerged the division of flow at junction is relatively unaffected by the changes in the downstream section of the branch channel.

Best and Reid (1984) undertook a study to create a relationship between flow parameters and separation zone dimensions for various confluence angle. Their results indicate that both length and width of separation zone increase with increasing discharge ratio, for the 90° confluence angle. For branching channels or intakes, result obtained from different researchers (Kasthuri and Pundarikathan 1987; Best and Reid 1984; Neary et al 1999) indicate that both length and width of the separation zone decrease with increasing the discharge ratio. Results obtained from the current 2D-numerical model for dimensions of separation zone were compared with Kasthuri and Pundarikathan's experimental (1987).

## 1 Experimental Investigation

Dimension of separation zone obtained from the current numerical model were compared with laboratory experiment results performed by Kasthuri and Pundarikathan (1987).

In their experimental set-up, the main channel was 6m long and the intake was 3m long, fitted at its midpoint. The width of both channels was 0.3m, the bed slope was zero and channels were 0.25m deep. The channel bed was finished with smooth cement plaster and walls were built from Perspex sheets.

In Kasthuri and Pundarikathan's experimental (1987) flows were subcritical during all runs and the Froude number in inlet varying from 0.1 to 0.4. They have presented relationships between the maximum non-dimensional length ( $S_L/b$ ) and non-dimensional width ( $S_W/b$ ) of the separation zone, and  $R=Q_b/Q$ . The results show both the length and the width of the separation zone decrease with increasing  $R$ .

## 2 Numerical Model Description

FLUENT is the CFD solver for choice for complex flow ranging from incompressible (transonic) to highly compressible (supersonic and hypersonic) flows. It Provides multiple solver options, combined

with a convergence-enhancing multi-grid method, FLUENT delivers optimum solution efficiency and accuracy for a wide range of speed regimes. (Fluent user guide 2003)

FLUENT solves governing equations sequentially using the control volume method. The governing equations are integrated over each control volume to construct discrete algebraic equations for dependent variables. These discrete equations are linearized using an implicit method.

Turbulent flows can be simulated in FLUENT using the standard K- $\epsilon$ , LES, RNG, or the Reynolds-stress (RSM) closure schemes. The model optimizes computational efficiency by allowing the user to choose between various spatial (Second-order upwind, first-order, QUICK) discretization scheme. We used second order upwind discretization scheme for Pressure, Momentum, Turbulent kinetic energy and turbulent dissipation rate and used SIMPLE algorithm for Pressure-Velocity Coupling Method.

## 3 Governing equations

The governing equations of fluid flow in rivers and channels are generally based on three-dimensional Reynoldes averaged equations for incompressible free surface unsteady turbulent flows as follows [2]:

$$\frac{\partial U_i}{\partial t} + U_j \frac{\partial U_i}{\partial x_j} = \frac{1}{\rho} \frac{\partial}{\partial x_j} \left[ \left( -P + \frac{2}{3} k \right) \delta_{ij} + \nu_T \left( \frac{\partial U_i}{\partial x_j} + \frac{\partial U_j}{\partial x_i} \right) \right] \quad (1)$$

There are basically five terms: a transient term and a convective term on the left side of the equation. On the right side of the equation there is a pressure/kinetic term, a diffusive term and a stress term.

In the current study, it is assumed that the density of water is constant through the computational domain. The governing differential equations of mass and momentum balance for unsteady free surface flow can be expressed as [8,9]:

$$\frac{\partial u_i}{\partial x_i} = 0 \quad (2)$$

$$\frac{\partial u_i}{\partial t} + u_j \frac{\partial u_i}{\partial x_j} = -\frac{1}{\rho} \frac{\partial P}{\partial x_i} + g_{xi} + \nu \nabla^2 u_i \quad (3)$$

Where  $t$ =time;  $u_i$  is the velocity in the  $x_i$  direction;  $P$  is the pressure;  $\nu$  is the molecular viscosity;  $g_{xi}$  is the gravitational acceleration in the  $x_i$  direction, and  $\rho$  is the density of flow.

As in the current study, only the steady state condition has been considered, therefore equation (2) to (3) incorporate appropriate initial and boundary conditions deployed to achieve equilibrium conditions.

The under-relaxation factors are chosen between 0.2 and 0.5. The small value of the under-relaxation factors is required for the stability of the solution of interpolation scheme.

Turbulent stresses in Reynolds-averaged equations can be closed using any of several existing turbulence models. No single turbulence model is accepted universally for solving all classes of problems but each model has certain advantages over the others depending on the type and the nature of the flow field to be simulated and the desired accuracy of results [2].

The Reynolds stress model (RSM) provides closure of the Reynolds-averaged Navier-Stokes equations by solving transport equations for Reynolds stresses and an equation for energy dissipation rate (four-equation for 2D flows and seven-equation for 3D flows). This turbulence model used in the present study. Since the RSM accounts for the effects of streamline curvature, swirl, rotation, and rapid changes in strain rate in a more rigorous manner than one-equation and two-equation models, it has greater potential to give accurate predictions for complex flows.

The exact transport equations for the transport of the Reynolds stresses,  $\overline{\rho u_i u_j}$ , may be written as follows:

$$\begin{aligned} \frac{\partial}{\partial t}(\overline{\rho u_i u_j}) + \frac{\partial}{\partial x_k}(\overline{\rho u_k u_i u_j}) = & -\frac{\partial}{\partial x_k}[\overline{\rho u_i u_j u_k} + p(\delta_{kj} u_i + \delta_{ik} u_j)] + \\ \frac{\partial}{\partial x_k} \left[ \mu \frac{\partial}{\partial x_k} (\overline{u_i u_j}) \right] - \rho \left( \overline{u_i u_k} \frac{\partial u_j}{\partial x_k} + \overline{u_j u_k} \frac{\partial u_i}{\partial x_k} \right) - \rho \beta (g_i \overline{u_j \theta} + g_j \overline{u_i \theta}) \\ + p \left( \frac{\partial \overline{u_i}}{\partial x_j} + \frac{\partial \overline{u_j}}{\partial x_i} \right) - 2\mu \frac{\partial \overline{u_i}}{\partial x_k} \frac{\partial \overline{u_j}}{\partial x_k} - 2\rho \Omega_k \left( \overline{u_j u_m} \varepsilon_{ikm} + \overline{u_i u_m} \varepsilon_{jkm} \right) + s_{user} \end{aligned} \quad (4)$$

Since flows through lateral intakes adjoining rivers and canals are turbulent and a very complex flow exists we use RSM turbulence model in this paper.

## 4 Boundary conditions

Appropriate condition must be specified at domain boundaries depending on the nature of the flow. In simulation performed in the present study, velocity inlet boundary condition is specified and set to 0.5m/s to provide similar Experimental Froude number; outflow boundary condition used for two outlets for all of runs. The length of the main and branch channel were chosen properly; therefore sufficient distance is provided between the junction and two outlets to ensure that the flow returned to the undisturbed pattern. Fig.2 represents the layout of the simulated main channel and intake.

Seven discharge ratios  $R=Q_b/Q$  equal to 0.2, 0.35, 0.45, 0.52, 0.65, 0.80 and 0.90 were used.

The no-slip boundary condition is specified to set the velocity to be zero at the solid boundaries and assumed to be smooth.

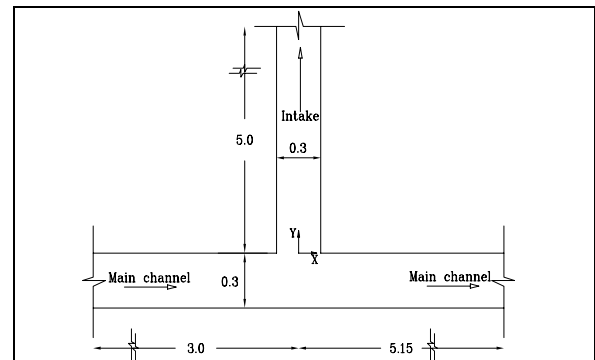


Fig2. Layout of main channel and intake

It is also important to establish that grid-independent results have been obtained. The grid structure must be fine enough especially near the wall boundaries and the junction, which is the region of rapid variation. Various flow computational trials have been carried out with different number of grids in x and y directions. It was found that results are independent of grid size, if at least 3550 nodes are used. Computational mesh is shown in Fig.3.

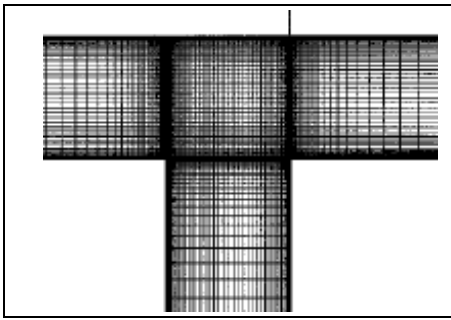


Fig.3. Computational geometry and grid

### 5 Results and Discussions

Figs. (4) to (5) presents the predicted variation of non-dimensional width and Length of separation zone in intake for different discharge ratios. The measurement of Kasthuri and Pundarikanthan (1987) is included for comparison. A good agreement is found between the experimental data and the present numerical results.

Results indicate that both length and width of the separation zone decrease with increasing discharge ratio. Separation zone reduces the effective width of the channel. It can be defined as the area of reduced pressure and re-circulating fluid with low velocities; therefore it has a strong sediment deposition potential in which sediment particles enter the branch channel. It can be seen that for a lower discharge ratio, more than 60% of the branch channel width is occupied by the re-circulating zone.

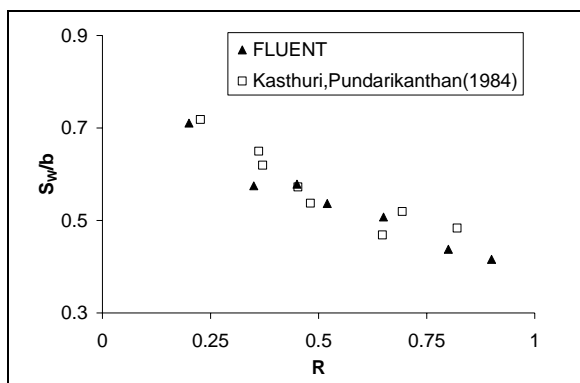


Fig4. Dimensionless width separation zone vs. Ratio of discharge

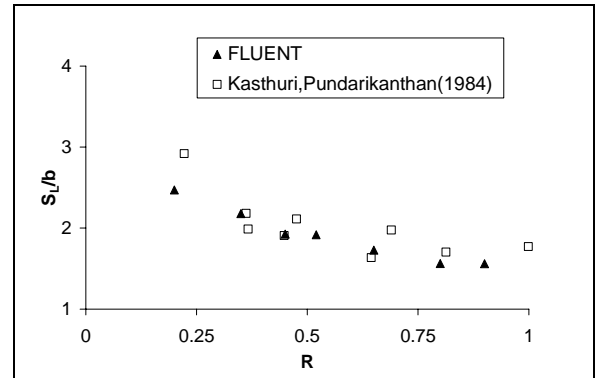


Fig5. Dimensionless Length separation zone vs. Ratio of discharge

Fig.6. shows that the contraction coefficient  $C_c$ , ( $C_c$ =effective width of lateral intake/width of intake), increases linearly as discharge ratio increases. This indicates that a smaller branch discharge  $Q_b$  results in a small effective width in the recirculation region of the branch channel.

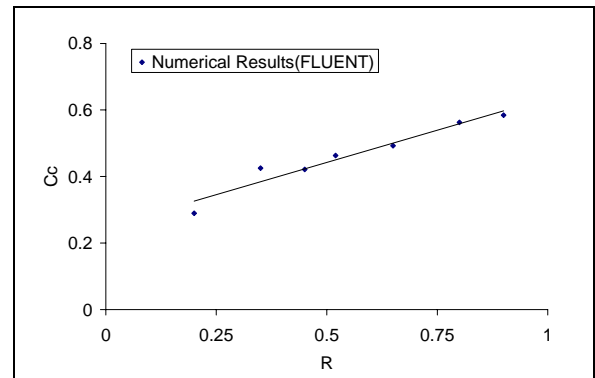


Fig6. Contraction coefficient in branch channel

### References

- [1] BEST J.L., REID., "Separation zone at open channel junction.", *Journal of Hydraulic Engineering*, Vol.110, No.11, 1984,pp.1588-1594
- [2] FLUENT user's guide manual-version 6.1., Fluent Incorporated, N.H., 2003
- [3] GRACE J. L., and PRIEST, M. S., "Division of flow in open channel junctions", Bulletin No. 31, Engineering Experimental Station, Alabama Polytechnic Institute, 1958.
- [4] KASTHURI B. and PUNDARIKHANTHAN N.V, "Discussion on separation zone at open channel junction.", *Journal of*

- Hydraulic Engineering*, Vol.113, No.4, 1987,pp.543-548
- [5] KRISHNAPPA G., SEETHARAMIAH K., "A new method of predicting the flow in a 90° branch channel.", *La Houille Blanche*, No.7, 1963
- [6] LAW S.W., "Dividing flow in an open channel." Ms Thesis, McGill Univ., Montreal, Canada, 1965
- [7] LAW, REYNOLDS, "Dividing flow in an open channel", *Journal of Hydraulic Div.*, Vol.92, No2,1966, pp.4730-4736
- [8] NEARY V.S., SOTIROPOULOUS F. and ODGAARD A.J., "Three-dimensional numerical model of lateral-intake inflows.", *Journal of Hydraulic Engineering*, Vol.125, No.2, 1999,pp.126-140
- [9] NEARY V.S. and ODGAARD A.J., "Three-dimensional flow structure at open-channel diversions.", *Journal of Hydraulic Engineering*, Vol.119, No.11, 1993, pp. 1223-1230
- [10] RAMAMURTHY A.S, SATISH M.G, "Internal hydraulics of diffusers with uniform lateral momentum distribution.", *Journal of Hydraulic Engineering*, Vol.113, No.3, 1987,pp.449-463
- [11] RAMAMURTHY. A. S., JUNYING Qu; and DIEP VO., "Numerical and Experimental Study of Dividing Open-Channel Flows.", *Journal of Hydraulic Research*, Vol.133, No.10, 2007, pp.1135-1144
- [12] SHETTAR A.S. and MURTHY K.K., "A Numerical study of division flow in open channels.", *Journal of Hydraulic Research*, Vol.34, No.5, 1996,pp.651-675
- [13] SRIDHARAN K., "Division of flow in open channels.", Thesis, Indian Institute of Science, Bangalore, India, 1966
- [14] TAYLOR, E.H. "Flow characteristics at rectangular open-channel junctions." *Trans. ASCE*, 109, 1944, pp. 893-902